Bioresource Technology 419 (2025) 132097

Contents lists available at ScienceDirect

Bioresource Technology

journal homepage: www.elsevier.com/locate/biortech

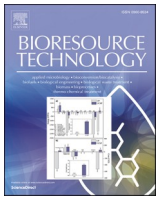

Assessment of temperature dynamics during methane oxidation in a pilot scale compost biofilter

Tania L. Gómez-Borraz [1], Yuly Vanessa Torres-Arévalo, Yovany Cuetero-Martínez, Armando González-Sánchez, Adalberto Noyola [*]

Instituto de Ingeniería, Universidad Nacional Autónoma de México, Circuito Escolar, Ciudad Universitaria, C.P. 04510 Ciudad de México, México

HIGHLIGHTS

- Biological CH_4 oxidation can generate thermophilic conditions in compost biofilters.
- CH_4 oxidation is performed efficiently at high temperatures by thermotolerant species.
- Sustained thermophilic conditions induced a shift of metabolism towards catabolism.
- Compost bed drying is likely the most critical parameter in decreasing CH_4 oxidation.
- Moisture monitoring and control are crucial for stable long-term CH_4 biofiltration.

GRAPHICAL ABSTRACT

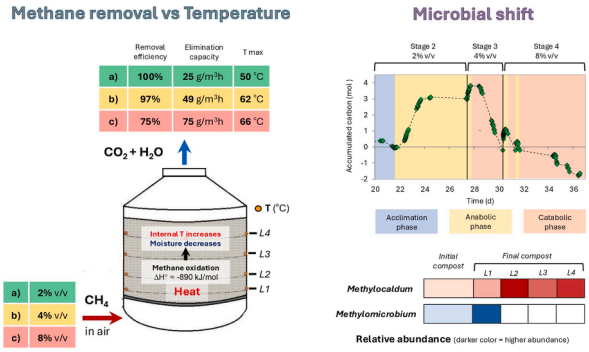

ARTICLE INFO

Keywords:
Biofiltration
Greenhouse gas mitigation
Methanotrophic bacteria
Moisture content
Thermophilic

ABSTRACT

Biological methane oxidation can sustain high temperatures in organic matrices, such as landfill covers and compost biofilters. This study investigates the temperature dynamics, methane removal efficiency, and microbial community responses in a pilot scale compost biofilter under three methane concentrations (2, 4, and 8 % v v^{-1} in air) with a 23-minute empty bed residence time. Complete methane removal was achieved at 2 %, with compost bed temperatures reaching 51 °C. At 4 % and 8 %, temperatures exceeded 60 °C, reducing methane removal efficiency to 97 % and 75 %, respectively, with maximum removal rates of 75 g $m^{-3}h^{-1}$. Thermotolerant *Methylocaldum* dominated at temperatures above 50 °C. Elevated temperatures shifted microbial metabolism from anabolism toward catabolism, likely due to thermal stress, as indicated by outlet gas profiles. These findings highlight the importance of optimizing operating conditions, such as moisture control and heat extraction, to balance thermal performance and microbial activity for effective methane biofiltration.

* Corresponding author.
E-mail address: noyola@pumas.ii.unam.mx (A. Noyola).
[1] Present address: James Watt School of Engineering, University of Glasgow, G12 8LT Glasgow, United Kingdom.

https://doi.org/10.1016/j.biortech.2025.132097
Received 4 October 2024; Received in revised form 7 January 2025; Accepted 17 January 2025
Available online 20 January 2025
0960-8524/© 2025 The Author(s). Published by Elsevier Ltd. This is an open access article under the CC BY license (http://creativecommons.org/licenses/by/4.0/).

1. Introduction

Methane (CH_4) is the second most predominant greenhouse gas (GHG) in the atmosphere. Its global warming potential (GWP, 100 years) is 27–30 times higher than carbon dioxide (IPCC, 2021). Methane production is both related to natural processes and anthropogenic activities. According to estimations from the last decades, up to 70 % of the total emissions come from direct human activity (Saunois et al., 2020), including waste treatment. Specifically, anaerobic treatment technologies for solid and liquid waste management produce methane that can be used for energy production (heat or electricity). However, biogas handling is accompanied by fugitive emissions, such as pipe leaks, inefficient collection or burning, and dissolved methane in anaerobic effluents, not to mention the free venting of landfills, wastewater treatment ponds, and small anaerobic reactors unable to maintain regular biogas production. The main characteristics of this type of emissions are their low methane concentration and their very variable flows. In recent years, methane biofiltration has emerged as a promising technology in order to tackle some of these fugitive emissions (Fjelsted et al., 2020; Huete et al., 2018; Turgeon et al., 2011). Biofiltration removes contaminants in a gas phase passing through a filter media containing microorganisms that carry out their metabolic process predominantly under aerobic conditions. The pollutants are transferred through convection and diffusion processes from the gas to the liquid phase in contact with an active layer of microorganisms. In particular, methane biofiltration uses aerobic methanotrophic microorganisms such as *Methylocaldum* and *Methylomicrobium* to oxidize methane into carbon dioxide, biomass, and water (Smith and Murrell, 2009; Tikhonova and Kravchenko, 2019, Takeuchi et al., 2014), based on the following chemical reaction:

$$CH_4 + 2O_2 \rightarrow CO_2 + 2H_2O + Heat \quad \Delta H^{\circ} = -890 \ \frac{kJ}{mol} \quad (1)$$

The understanding of the biological oxidation process of methane and the factors influencing its operation have been widely addressed by carrying out experiments, mainly at laboratory scale (Gómez-Borraz et al., 2017; Gomez-Cuervo et al., 2016; Nikiema et al., 2005). However, these results may not be extrapolated and applicable on a real scale, considering the effect of variables, such as external temperature changes or rainfall, in open, full-scale biofilters (Hettiarachchi et al., 2011).

As a biological treatment, microbial activity is highly influenced by physical parameters such as temperature. The relevance of the effect of temperature on methane oxidation in a biofilter should be approached by considering the influence of external and internal temperature changes. The external temperature is related to seasonal changes and variations between day and night, which can be modified by the biofilter design and type of installation (insulated, covered, or outdoors). The internal temperature is associated with the generation of metabolic heat from microbial activity. The temperature gradient between the biofilter and the environment causes heat loss or gain through the walls. For this reason, recent research using pilot- and real-scale reactors included temperature monitoring in the packing bed. Huete et al. (2018) described a compost bed biofilter (0.34 m^3) to treat a low methane concentration gas flow (2–4 %) desorbed from an anaerobic effluent. Results of temperature monitoring showed an increase in the compost bed temperature with a mean value of 50 °C during the stable operation period. Similarly, Fjelsted et al. (2020) studied an open-bed compost biofilter (18 m^3) to treat methane from an old landfill. They reported sustained high temperatures inside the compost bed, close to 50 °C even during winter. Methane oxidation, being an exothermic reaction ($\Delta H^{\circ} = -890$ kJ mol^{-1}, Salahudeen et al., 2022), is the main heat source; however, the contribution of all heat sources in a real methane biofiltration process is unclear, which also includes ambient conditions such as solar radiation and ambient temperature.

The relevance of controlling the temperature within the packing material remains a knowledge gap in the literature. That is mainly because a rise in temperature causes both drying of the filter bed and a decrease in the gas solubilities, which consequently reduces the already limited mass transfer rate and, therefore, its availability for microbial uptake and reaction. In this regard, the low methane solubility in water and its diffusion within the biofilm has been identified as the limiting step during methane biofiltration (Gómez-Borraz et al., 2017), which is accentuated at higher temperatures. Conversely, on the other hand, it can also promote a change in the microbial community for survival and acclimation, achieving a more effective conversion under thermophilic conditions (Scheutz et al., 2017). There are several reports about the causes of the temperature increase in biofilters (Huber-Humer et al., 2009); among them, Gómez-Borraz et al. (2022) simulated several operating conditions using a calibrated mathematical model. They found that the prevailing high temperature at the center and upper zones of the biofilter inhibited their methanotrophic biomass, so methane oxidation was primarily accomplished at the inlet (bottom) and wall zones. To date, no systematic experimental studies have focused on the understanding of the phenomena in a physical prototype. Therefore, this work aims to determine the temperature dynamics and its effect in the compost bed at three different methane loading conditions, to better understand the causes and implications of the temperature increase in the performance, operation, and changes in the microbial communities during methane biofiltration at pilot scale.

2. Materials and methods

The study was carried out at the main Campus of the National Autonomous University of Mexico (UNAM) from October to December 2020. The system was installed on the roof of the Environmental Engineering building at the Institute of Engineering, UNAM campus (México City), under a 75 % shade cloth cover.

2.1. Compost biofilter set-up

The biofilter was made from a commercially available 0.45 m^3 high-density polyethylene (HDPE) storage tank (1 m height, 0.85 m inner diameter). The filter was packed with 0.3 m^3 of mixed compost obtained originally from the producing facility at UNAM, receiving plant and food waste collected from the university campus. The mixture was integrated with three different kinds of compost: mature, fresh, and used in a previous study for methane and H_2S removal, in a volume ratio of 4:1:1, respectively. As a fraction of the compost was already acclimated to methane feeding, no inoculation of methanotrophic bacteria was considered. The compost was manually homogenized and moistened before its use in the biofiltration experiment.

Only air was fed to the biofilter during the first stage to start the operation of the biofiltration system. The addition of methane occurred after day 15. The pollutant gas stream, 0.78 m^3/h, was made by mixing air and methane to reach the desired final concentration and an empty bed residence time (EBRT) of 23 min. Air was pumped using a diaphragm pump through two humidifier columns connected in series (0.9 m height, 0.05 m diameter, each), one third filled with volcanic rocks, and tap water up to 0.65 m height. The excess moisture was removed in a water trap. Methane was supplied from a compressed gas cylinder (Praxair, 99 % v v^{-1}l), and the flow was regulated and monitored using a peristaltic pump, needle valve, and rotameter. The mixture of both gaseous streams was done in a separate column before entering the biofilter (Fig. 1). The differential pressure was measured using a water column manometer. The biofilter included a 10 cm-height chamber at the bottom to allow gas distribution and leachate collection and drain. A couple of plastic film circular baffles (5 cm wide) were installed at the inner wall at 0.2 and 0.4 m of the packed bed height to prevent gas channeling next to the biofilter wall. A lid captured the treated gas at the top of the biofilter.

Additionally, a network of 30 temperature sensors (LM35, Texas Instruments, USA) was placed at the inlet (1 item) and outlet (1 item) gas lines and distributed in the compost bed (28 items). The temperature

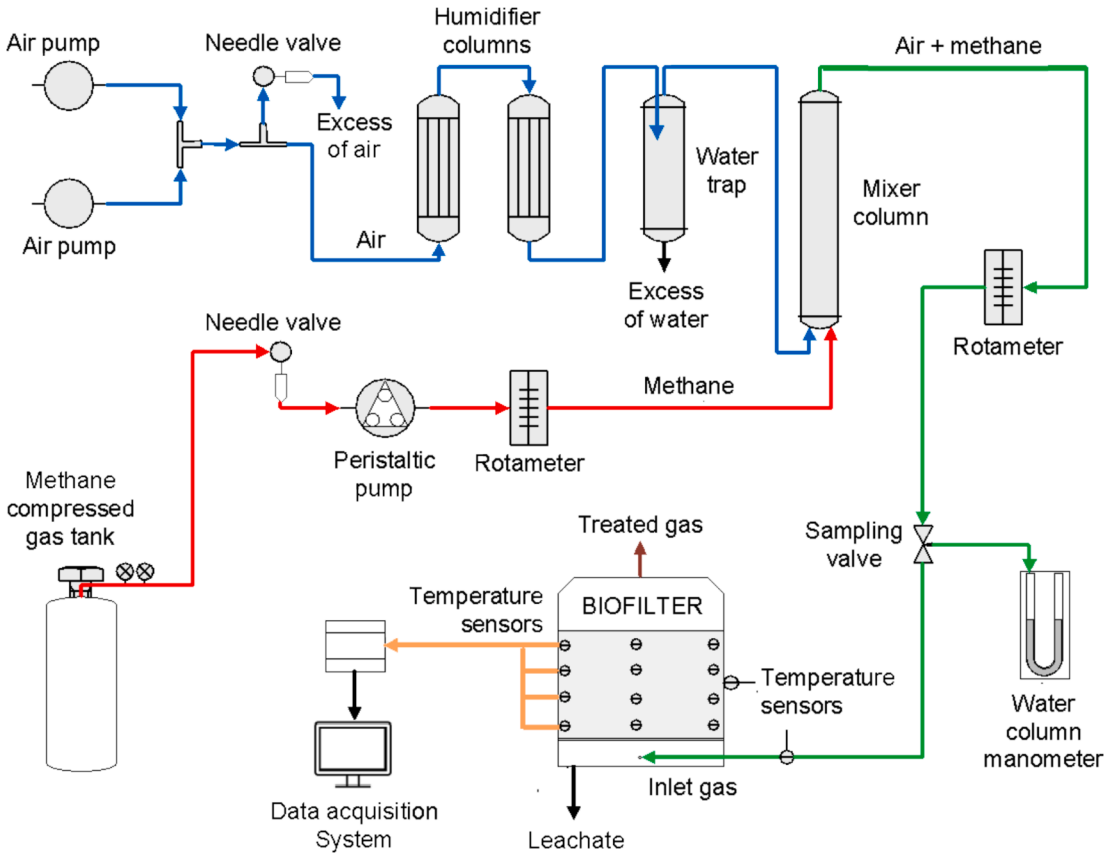

Fig. 1. Experimental arrangement of the pilot-scale biofiltration system.

sensors within the compost were arranged in 4 different levels: 5 cm (L1), 15 cm (L2), 35 cm (L3), and 50 cm (L4) from the supporting mesh at the bottom (inlet) of the biofilter. At each level, 7 sensors were allocated at the 4 cardinal points, the radial center and 2 more inner points (see supplementary material, Fig. S1). These data were collected every 5 min and stored using a data acquisition card model U3-LV (LabJack Co., USA) and a microcomputer Raspberry Pi 3 model B+ (UK).

2.2. Packing material characterization

The pH, apparent density, and porosity were estimated from the initial compost mixture. The pH was measured following the procedure reported by Blakemore et al. (1987) using a pH probe (Van London Phoenix Co., USA). Dry and wet apparent densities were calculated as the dry or wet mass ratio per volume unit of moistened compost. The compost porosity was estimated as described by (Gómez-Borraz et al., 2017).

The moisture content (MC) was determined at the beginning and end of the experiment. For the initial MC, a compost sample (15 g) was taken from the mixed compost before starting the operation in the biofilter. The final MC was estimated from two samples (15 g each) collected at 20 cm from the bottom of the compost bed (halfway between sensors levels 1 and 2, at the center and close to the biofilter wall), complemented with a third sample at the top of the compost bed. The MC was evaluated based on the weight differences after drying the samples at 105 °C for 24 h. During the experiment, in addition to the humidification of the gas inlet, a limited volume of tap water (3.72 L) was added manually at the top of the biofilter (see supplementary material, Table S1).

2.3. Biofiltration evaluation

The operational performance of the biofilter was assessed with the removal efficiency (RE), the elimination capacity (EC), and the mineralization ratio of methane (described in section 2.4). The RE is defined as the percentage of the initial pollutant concentration that is removed by the system, whereas the EC is the mass of the compound removed per m^3 of the reactor (packed bed) per time unit. In this work, the biofilter performance was evaluated at three methane loads (ML) and two only-air feeding conditions (initial and final stages, 1 and 5), as shown in Table 1. The methane loads and empty bed residence time (EBRT) were chosen according to previous work on removing methane desorbed from an anaerobic effluent at a pilot scale (Huete et al., 2018). The methane concentration in the air for the three methane stages (2, 3 and 4) were 2, 4 and 8 % v v^{-1}, respectively. Each stage duration relied upon the stabilization of the methane removal rate by the biofiltration system, measured in terms of the methane elimination capacity (g $m^{-3}h^{-1}$) and removal efficiency (%). Gas samples were taken from the inlet and outlet sampling points and stored in 10-L Tedlar bags. The gas composition,

Table 1
Experimental conditions to evaluate methane removal at three different methane inlet loads.

Stage	Methane concentration (% v v^{-1})	Methane load (g $m^{-3}h^{-1}$)	Gas flow (m^3/h)	EBRT (h)	Duration (h)
1	0	0	1.02 – 1.14	0.27 – 0.30	360
2	2.1 ± 0.2	26.2 ± 2.6	0.78	0.38	288
3	4.0 ± 0.1	51.4 ± 2.1	0.78	0.38	72
4	8.0 ± 0.4	102.6 ± 5.7	0.78	0.38	144
5	0	0	0.78	0.38	36

including methane, carbon dioxide (CO_2), oxygen (O_2), and hydrogen sulfide (H_2S), was measured using a handheld gas analyzer (Biogas 5000, Landtec).

Pressure drop, a relevant monitoring parameter for biofilter operation, was recorded using a water column manometer located at the inlet of the biofilter during the whole experiment. The water balance in the system was estimated on the 38-day of operation, as shown in Equation 2, considering the mass of water measured in the compost (initial and final moisture content, W_{bed_init} and W_{bed_end}), the moisture content in the gas stream assuming a 100 % water saturation (W_{inlet_gas} and W_{outlet_gas}), the sporadic manual addition of tap water at the top of the compost bed (W_{add}), the water produced by microbial activity ($W_{reaction}$), and the recovered leachate ($W_{leachate}$).

$$W_{bed\_init} + W_{inlet\_gas} + W_{add} + W_{reaction} - W_{bed\_fin} - W_{outlet\_gas} - W_{leacheate} = 0 \quad (2)$$

The water amount in the saturated gas streams was estimated using the ideal gas law, considering their temperature (inlet and outlet) and water vapor pressure within the Antoine equation (Eq. 3); where P_i represents the vapor pressure for water, and A_i, B_i, and C_i, the component-specific constants related to the vaporization, enthalpy, and entropy.

$$log_{10}P_i = A_i - \frac{B_i}{(T+273.15)-C_i} \quad (3)$$

Additionally, the amount of water generated by the biological reaction was estimated based on the methane removed according to the accomplished EC.

2.4. Carbon fate

To evaluate the fate of carbon in the system, the uptake and release of this element were estimated through the changes of methane and CO_2 at the inlet and outlet of the biofilter, during stages 2 to 4, so the accumulated molar values for methane consumption and CO_2 production were computed for the full experimental period. Besides, to assess the carbon mineralization ratio in the compost biofilter, the O_2 and methane consumption and CO_2 production were calculated based on the inlet and outlet gas composition and compared to the stoichiometric ratio for the methane oxidation reaction (Eq. 1), being 2 for O_2/CH_4, and 1 for CO_2/CH_4 considering complete mineralization of the removed methane.

2.5. Microbial community analysis

Samples of the initial (IC) and final compost (FC) were analyzed to compare the changes in of the microbial community after exposing the biofiltration system to methane and the resulting thermophilic temperatures. Two days after the completion of the experiment, grab samples were taken at four different heights of the compost bed: 5, 15, 35 and 50 cm and close to the filter wall; the samples were named L1, L2, L3 and L4, respectively. The DNA extraction was performed using the PowerSoil® DNA Isolation Kit-QIAGEN (QIAGEN, Germany) and following the manufacturer's instructions. With respect to the metataxonomic analysis for characterization of microbial communities; the samples were then sent to the Center for Comparative Genomics and Evolutionary Bioinformatics at Dalhousie University, Canada, where the massive sequencing of full 16S rRNA gene was performed with a PacBio Sequel II platform (Pacific Biosciences, USA). The bioinformatics analysis was done with the software QIIME2 version 2021.8 (Bolyen et al., 2019) and the pipeline of Comeau et al. (2017) available at https://github.com/LangilleLab/microbiome_helper/wiki using SILVA 138 database (Quast et al., 2013) as reference. Full 16S rRNA libraries are available in BioProject PRJNA1068161 of NCBI.

3. Results and discussion

3.1. Initial compost characterization as packing material

The initial values of pH, porosity and moisture of the compost were 7.32, 0.5 %, and 47.3 %, respectively. These values are in accordance with previous reports of compost material for methane biofiltration (Gómez-Borraz et al., 2017; Morgan-Sagastume et al., 2003). Whereas for the wet and dry apparent density of the compost bed, the values obtained were 0.64 g/ml and 0.33 g/ml, respectively, which are in the range proposed by (Agnew and Leonard, 2003). Moreover, the flat temperature profiles inside the biofilter during the first 15 days of the operation fed with ambient air, together with the absence of CO_2 in the outlet ($\leq$ 0.1 % v v^{-1}), evidenced that no relevant biological process was taking place and that the compost was mature, with no significant endogenous substrate.

3.2. Methane biofiltration performance evaluation

3.2.1. Elimination capacity and removal efficiency

Fig. 2 shows the biofilter performance during the three methane loads deployed during stages 2 to 4. Fig. 3 shows the relation between the ML and the EC for the biofiltration system. Once the methane was added to the system (day 15), the microbial community went through an acclimation period of a few days, exhibiting a presumably early pulse-type activation on day 17. On day 21, after 6 days of methane being fed to the system, the biofilter started consistently removing methane, showing an increase in the EC values from 1.3 to 5.3 $gCH_4\ m^{-3}h^{-1}$. From day 22 onwards, the EC gradually increased to reach its highest value, with a mean ML of 25 $\pm$ 1.8 $gCH_4\ m^{-3}h^{-1}$, and 100 % methane removal on day 23. From day 24 to 27, the system remained stable, removing all the methane fed to the system.

In stage 3, the ML doubled for an average of 51.4 $\pm$ 2.0 $gCH_4\ m^{-3}h^{-1}$, and the RE was reduced to 97.5 $\pm$ 1.7 %, representing an EC of 50.1 $\pm$ 1.6 $gCH_4\ m^{-3}h^{-1}$. For stage 4, where the ML was four times higher than stage 2 (102.6 $\pm$ 5.7 $gCH_4\ m^{-3}h^{-1}$), the average RE in the system decreased drastically to 73 $\pm$ 8.7 % with an EC of 75.8 $\pm$ 8.7 $gCH_4\ m^{-3}h^{-1}$. These values are similar to other studies for methane removal using compost biofilters. Streese and Stegman (2003) reported EC of 63 $gCH_4\ m^{-3}h^{-1}$ when the ML was 112 $gCH_4\ m^{-3}h^{-1}$ but fed with lower methane concentration (0.2 and 2.5 % v v^{-1}). Meanwhile, an average EC of 42 $gCH_4\ m^{-3}h^{-1}$ from 4.3 % v v^{-1} methane concentration was achieved in a similar pilot-scale biofilter under the same EBRT (Huete et al., 2018).

Overall, the results demonstrated the system's robustness in treating low-concentration methane-air streams at moderate EBRT and no oxygen limitation (<9.5 % v v^{-1} methane in air, representing a molar ratio of 2 $molO_2\ molCH_4^{-1}$). The system could reach almost complete methane depletion when the methane load was below 60 $gCH_4\ m^{-3}h^{-1}$. However, at higher volumetric mass flow (100 $gCH_4\ m^{-3}h^{-1}$), the biofilter efficiency was reduced to an average of 75 %, more likely due to a reaction limitation in the compost bed, triggered by the temperature increase affecting the entire filter media, including the upper level. Higher temperature conditions increase water evaporation, resulting in dryer compost and reduced water activity, impacting biological reactions; moreover, it also decreases the solubility of gases in water, affecting gas/liquid transfer and methane diffusion in the biofilm (Bian et al., 2021; Gómez-Borraz et al., 2021). In this regard, Gómez-Borraz et al. (2017), based on a lab scale compost biofilter treating 4 % methane in air at mesophilic temperatures, found that diffusional mass transport in the biofilm was the limiting step over the biological reaction. Reducing the methane solubility in the water fraction of the compost may thus be the leading cause of the decrease in the removal efficiency at stage 4.

3.2.2. Temperature effect

Fig. 4 presents the temperature profile measured during stages 2 to 5,

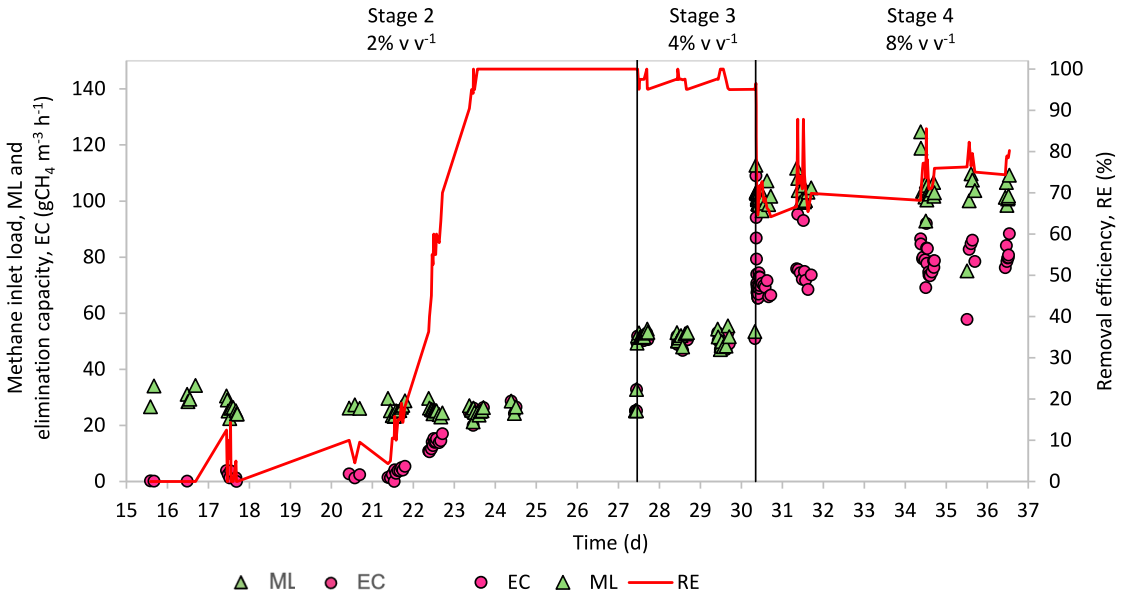

Fig. 2. Methane load (ML), elimination capacity (EC), and removal efficiency (RE) at an EBRT of 0.38 h for the three experimental stages fed with methane.

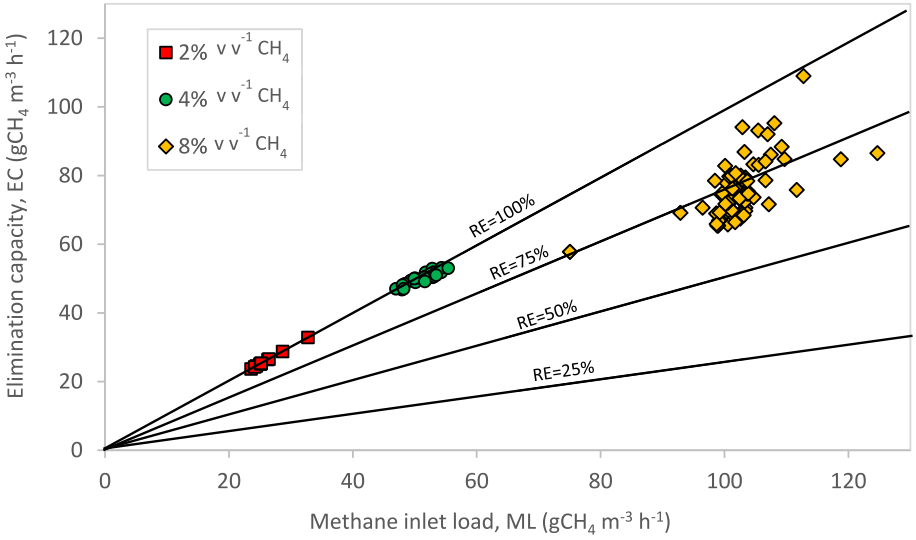

Fig. 3. Elimination capacity (EC) achieved at different methane inlet concentrations (% v v^{-1}) and resulting methane loads (ML) at an EBRT of 0.38 h, with their corresponding removal efficiency (RE).

using only the thermocouples located at the center of the biofilter for each level. It is evident that once methane is replaced by air in the system, the temperature inside the filter bed rises due to the microbial metabolism related to methane uptake (stage 2) and decreases when methane feeding is stopped (stage 5). Recent studies suggest that in a compost filtration bed, the temperature increase is caused by two heating biological-related generation processes: the heat generated during the catabolic conversion of methane into CO_2 and the natural decomposition of the compost organic matter (Scheutz et al., 2017; Pearce, 2023), being the latter negligible when mature compost is used.

At each stage, the radial center of the biofilter at the four height levels reached the highest temperature of the corresponding level. Throughout the first methane-fed condition (stage 2) with 2 % v v^{-1} methane in air, level 2 (15 cm from the inlet) reached 50 °C after the biofilter attained a semi-steady state operation with complete methane removal. Then, in stage 3 (4 % v v^{-1} methane in air), the EC increased to ~ 50 gCH_4 $m^{-3}h^{-1}$, resulting in temperature rises in all levels above 0.15 m but still maintaining nearly 100 % removal as in the previous stage. In this case, level 3 (at 0.35 m) showed the highest temperature, up to 65 °C, while level 4 stayed below 50 °C. A similar behavior was found by Fjelsted et al. (2020) during diluted landfill gas oxidation (methane concentration from 4.4 to 9.2 v v^{-1}) in a pilot-scale biofilter (18 m^3), where sustained average temperatures of 50 °C were recorded.

At stage 4, the overall removal efficiency was reduced when methane concentration increased to 8 % v v^{-1}, which is close to the stoichiometric balance in the methane oxidation reaction with air, corresponding to 9.5 % v v^{-1} methane and 19 % v v^{-1} oxygen (71.5 % v v^{-1} nitrogen) (Eq. 1). During this stage, all levels showed stable mean temperature values, except for level 2, in which temperature gradually decreased from 57 °C to 48 °C at the end of the stage. There is no evident explanation for the decoupling of the similar temperature behavior of levels 2 and 3 shown during the previous stages. At stage 4, the entire system operated under substrate saturation conditions, such as level 1 during the whole experimental period. However, MC (see section 3.2.4) was adequate at

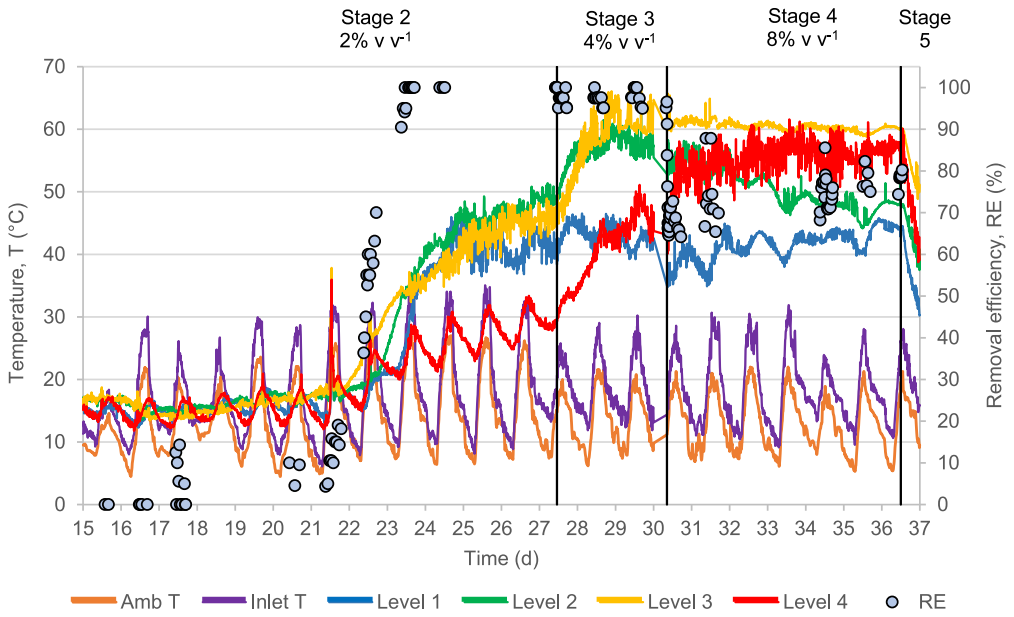

Fig. 4. Overall removal efficiency and temperature profiles during stages 2–5 recorded at the radial center of the biofilter at different levels: 1 (0.05 m), 2 (0.15 m), 3 (0.35 m), 4 (0.5 m).

the lowest level due to the humidity in the inlet gas, as well as at the highest level due to water condensation on the filter cover. Presumably, the methanotrophic biomass at level 2 was affected by a low MC, an effect accumulated during the experiment. It is possible that the generated metabolic heat and the convective transport of water vapor, dried the middle section of the biofilter, and level 2 in particular, reducing the microbial activity in this zone, as discussed by van Lith et al. (1997) and Morales et al. (2003). The temperature rise promotes a higher water evaporation rate in the packing material, decreasing the gases' solubility in the liquid phase and, consequently, the gas/liquid transfer rate of methane and oxygen in the biofilm (Bian et al., 2021). Stein and Hettiaratchi (2001) observed an increase in methane removal when they increased the water content in the filter bed after 60 days of operation, supporting the importance of moisture monitoring and control in biofiltration systems (Bonilla-Blancas et al., 2024). On the other hand, level 4 presented a temperature rise to 60 °C, suggesting an activation of a previously inactive zone in the compost bed, due to limited access to methane at such level during stages 2 and 3. According to Gómez-Borraz et al. (2022), the highest-temperature zones do not necessarily correspond to the highest-metabolic activity areas. As a matter of fact, once the high temperature causes undesirable conditions in some zones of the compost bed, usually the center in a cylindrical reactor, the biologically active zone displaces to an area with more favorable temperature and moisture conditions (e.g. close to the reactor wall).

The temperature of the compost at the center of level 2 and 3 presented a pattern independent of fluctuations in the inlet temperature. In contrast, the pattern of level 1 was influenced by the inlet variations, but in an inverse behavior, after the temperature increase, ending on day 24. An explanation is that low ambient temperature during the night, and therefore lower temperatures of the inlet gas, led to more favorable conditions for the methanotrophic bacteria located below level 1 (5 cm height), increasing their metabolic activity and thus heat generation. This, in turn, increases the temperature at level 1, which is also influenced by the convective heat transport of the gaseous flow, resulting in a daily cyclic pattern. In the case of level 2 (at 15 cm), the daily temperature pattern was only partially visible in stage 4, when a possible decrease in microbial activity occurred due to a reduction in the moisture content in this zone, as previously discussed. Regarding level 4, the influence of ambient temperature fluctuation was evident in stage 2, due to the proximity of the headspace and biofilter cover, and the absence of methanotrophic activity caused by the low loading conditions at this level due to full (stage 2) or almost full (stage 3) methane removal at lower levels.

Fig. 5 shows an example of the radial temperature profiles, based on 5 equidistant thermocouples, in the compost bed at the four different levels during stages 2 (day 25), 3 (day 29) and 4 (day 35) at 6:00, 13:00 and 18:00 h. The lowest ambient and inlet gas temperatures were registered at 6:00 h, while the highest temperatures recorded were at 13:00 h. Temperature is shown using the horizontal (radial) distance of the biofilter, where zero represents the biofilter wall facing north, and 0.85 m the opposite side facing south, which received more solar radiation during the day. The highest radial temperatures recorded were found at or close to the center of the biofilter, regardless of the level. The parabolic shape is due to the heat exchanged at the biofilter wall between the compost media and the ambient temperature, which cooled the compost located at that area (Gómez-Borraz et al., 2022). Even so, temperatures exceeding 30 °C at the walls were found in the intermediate levels (2 and 3), sometimes well above the ambient and inlet gas temperatures, as in the case of 6:00 h, when those temperatures were only between 6 to 7 °C and 10 to 13 °C, respectively. The higher gas inlet temperature compared to the ambient was caused by the heat transferred from the air feeding pump.

Regarding the temperature profile along the biofilter height, the central zone of the biofilter (center of levels 2 and 3) may be considered thermally isolated from the outside. The heat produced in the perimeter and at the base (inlet) of the biofilter is primarily carried by convection in a vertical (axial) direction, with a lesser amount being conducted in a horizontal (radial) direction. As a result, the heat builds up in levels 2 and 3 due to the compost's heat capacity until it reaches the high values shown in Fig. 5. At the upper part of the biofilter (level 4), where heat exchange is favored as the compost is in contact with the headspace of the biofilter, lower temperatures were recorded, except for stage 4, receiving the highest methane feed (8 % v v^{-1}). In this case, two important changes were introduced: methane reached the compost at the upper level, triggering the metabolic activity of the methane oxidizers at that zone, and the high methane load produced additional metabolic heat in the whole system, which was transported by convection to the upper part of the biofilter, increasing the outlet gas temperature from 16 °C (Stage 2 at 6:00 h) to 42 °C (Stage 4 at 13:00 h).

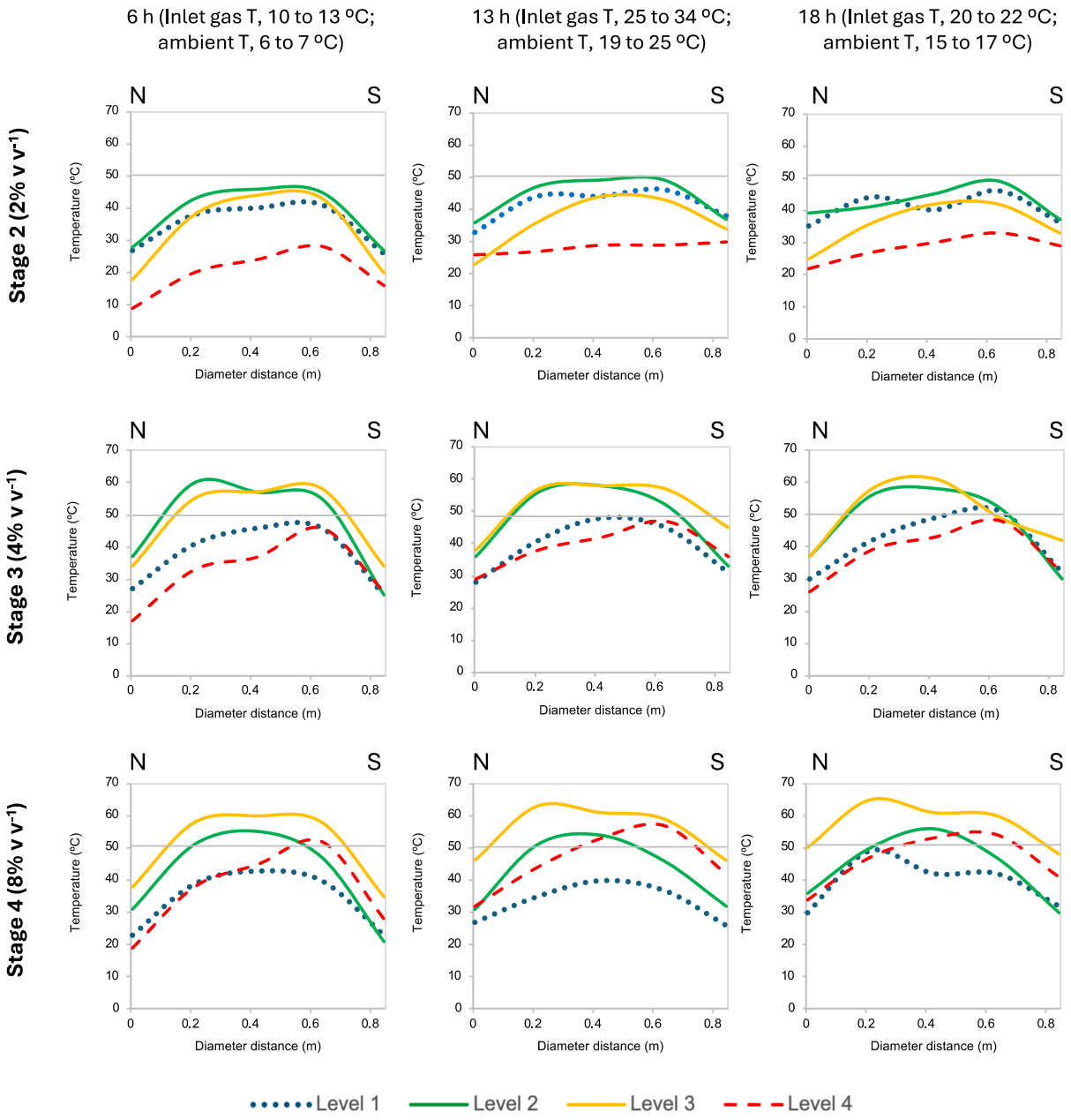

Fig. 5. Temperature profiles at different levels across the biofilter during stages 2 (day 25), 3 (day 29) and 4 (day 35) and corresponding ambient and inlet temperatures. The zero in the diameter distance represents the biofilter wall facing north (N), while 0.85 m represents the opposite side facing south (S).

It may be noticed that level 2 consistently reached the highest temperature during stage 2, while at stage 3, level 2 and 3 showed similar behavior, shifting to level 3 at stage 4, as presented before. This data supports the previous discussion on the unexpected temperature drop of level 2 during stage 4, as this level was subject to the highest temperatures for most part of the experiment, not being favored by the water content from the inlet, thus increasing compost drying. The low MC of the compost sample at the center of level 2 at the end of the experiment (27.2 %, presented below) is consistent with this explanation.

Lastly, during stage 5 (no methane feeding), the cooling of the compost bed relied mainly on the airflow (forced-convection heat transport). Additionally, conductive transport contributed to the reduction of the internal temperature, which depends on the thermal conductivity of the compost and the temperature gradient between the inside and outside of the biofilter. During the cooling period, the concentration of gases at the outlet was measured (see supplementary material, Fig. S2). Temperature at level 3 dropped from 60 °C to 24° after 46 h, taking the longest time (nearly 3 days) to reach ambient temperature (data not shown). At stage 5, methane concentration at the outlet decreased rapidly; in 25 min (1.08 times EBRT), it dropped from 1.6 % to 0 % v v^{-1}. On the other hand, the CO_2 concentration had a slower decrease, taking 21 h (54.7 times EBRT) to go from 6.5 % to 0.4 % v v^{-1}, still above its concentration in ambient air (0.04 % v v^{-1}). Mass balance considerations in the gas and liquid-biofilm phases may explain the different behavior of methane and CO_2. In the case of methane, once the gas stream is changed to air, the mass transfer from the gas phase to the liquid phase becomes zero. In contrast, the gradient for the opposite direction is insignificant due to the very low concentration in the liquid phase (~1.2 mg/L). Therefore, methane transportation is merely related to the gas convective flow through the compost bed. Hence, the time taken for methane to reach zero concentration value at the system outlet is essentially the EBRT. However, for the case of CO_2, at least three

additional biological processes can occur simultaneously for residual CO_2 production: endogenous respiration from compost material, residual methane oxidation in the biofilm, and residual metabolites from methanotrophs (e.g. methanol and formaldehyde). On the other hand, because of its greater solubility in water, the CO_2 will desorb slower from the compost to the gas phase, if compared to the less soluble methane. Therefore, the outlet CO_2 concentration decreases more slowly compared to the outlet methane concentration and will not necessarily reach the ambient concentration (0.04 % v v^{-1}) in short term.

3.2.3. Pressure drop performance

The pressure drop for the filter bed was recorded using a water column differential manometer. Fig. 6 shows the relation between the gas flow and pressure drop in the system. For equal gas flows, as is the case of this work in stages 2 to 5, the pressure changes can indicate compaction of the support bed, channeling that will allow preferential flows or biomass growth reducing the bed porosity (Morgan-Sagastume et al., 2003). During stage 1 (days 0 to 14), the biofilter operated at an EBRT between 16 and 18 min, so the higher pressure drop registered at such condition, compared to the subsequent stages (EBRT 23 min), would result from the higher flow applied in stage 1.

The average flow of stages 2 to 4 was 0.77 ± 0.01 m^3/h. From stage 2 to 3, there was a slight average increase in pressure from 13.9 ± 1.2 $cmH_2O\ m^{-1}$ to 16.3 ± 0.3 $cmH_2O\ m^{-1}$, while in stage 4, a smaller increase in the mean value ($\Delta = 1\ cmH_2O\ m^{-1}$) was observed when the methane concentration was doubled at 8 % v v^{-1}. In general, the trend of the pressure variation in the compost bed was positive and linear in the three stages with methane feeding. Huete et al. (2018) reported higher pressure drops for a similar biofilter (0.3 m^3, 0.6 m compost bed height and 23 min EBRT): 29 $cmH_2O\ m^{-1}$ during the first 12 days of operation, reaching 37 $cmH_2O\ m^{-1}$ after 57 days ($\Delta = 8\ cmH_2O\ m^{-1}$).

For stage 5, a reduction in pressure (5 $cmH_2O\ m^{-1}$) was recorded despite maintaining the EBRT and gas flow velocity. In general, it can be assumed that preferential flow channels did not form in the compost bed, as there was no reduction in the pressure drop during the operation. On the contrary, the increasing trend may be associated with the compaction of the bed and/or biomass growth. Another assumption that can be made is that the pressure drops during the methane feeding stages, were, in part, due to the high temperature inside the compost bed, if compared to ambient conditions. Gases expand with temperature, increasing the pressure drop due to the higher flow resistance of the compost media. That would explain why when the gas composition changed, and there was no more methane in the system, the inner temperatures started dropping, and so did the pressure drop in the biofilter.

3.2.4. Moisture content

At the end of the experiment, the moisture content was determined with the average values at three sampling points, two at level 2, where most of the methanotrophic activity presumably occurred, and the other at the top of the compost bed. The first couple of sample points were located, one next to the biofilter wall and the other in the center, with MC values of 41.69 ± 1.25 and 27.20 ± 0.73 %, respectively. In contrast, the sample from the top of the compost bed presented a higher value of 54.79 ± 0.63 % compared with the initial moisture content of 47.3 %. The latter was expected as the manual water addition (see supplementary material, Table S1), although scarce, was applied at the top of the compost bed, but the main reason can be related to the condensed water dripping from the biofilter cover. Bonilla-Blancas et al. (2024) and Morales et al. (2003) recommended to operate biofiltration systems around 40 to 50 % of moisture for hydrophobic compounds removal, such as methane. Lower humidity values will result in restricted microbial activity, while higher values will limit the gaseous contaminant transfer rate into the biofilm (Bonilla-Blancas et al., 2024). Therefore, the results obtained here highlight the need for considering moisture control, especially as temperature rise favors water evaporation. It is noteworthy that drying negatively influenced the microbial activity in areas with higher temperatures (Morales et al., 2003), such as the center of levels 2 and 3 (Fig. 5), partially explaining the decrease in the EC during stage 4 and the corresponding temperature reduction at the center of level 2, as previously discussed.

Table 2 includes an overall estimate of the water balance for the system. The moisture content in the compost represents nearly 80 % of the initial and final water inventory. A very limited quantity of leachate (60 mL) was recovered from the bottom of the biofilter at the end of the experiment during stage 5 (cooling stage). The water balance shows a deficit of 12.6 %, referring to the initial values and the system water inputs. Nevertheless, during the final stage, the compost demonstrated a moisture profile that was apparently linked to the operational temperature, and water condensation was observed at the top of the reactor. Therefore, the moisture content estimated with three samples was not a representative average for the entire compost bed, and the final moisture value was likely underestimated. Furthermore, the water from the methane oxidation reaction is overestimated since complete mineralization was considered for its calculation, not considering the fraction used for biomass growth. However, this item is not significant (237 mL

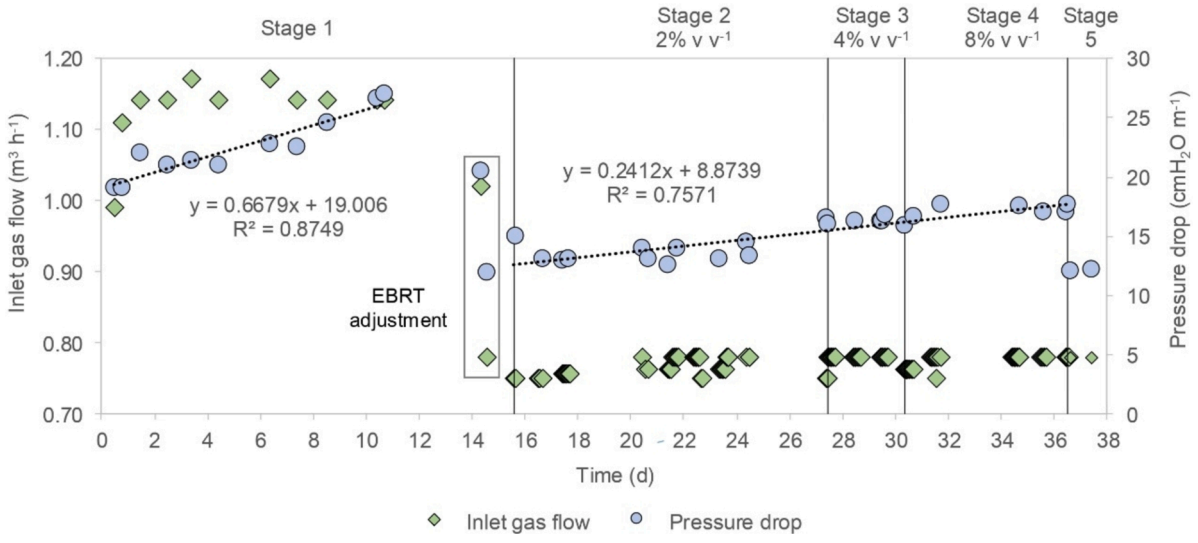

Fig. 6. Inlet gas flow and pressure drop correlation for the complete biofilter operation.

Table 2
Water balance in the compost biofilter at the end of the experiment.

Water source	Total water (L)
Inlet	
Initial moisture content in the compost mixture (47.3 %)	90.9
Water-saturated total inlet gas flow (after humidifier columns)	14.6
Manual tap water addition (see supplementary material, Table S1)	3.7
Water generated due to biological methane oxidation reaction	11.8
Total	**121.1**
Outlet	
Final moisture content in the compost mixture (41.2 %)	79.2
Water-saturated total gas flow treated (assuming 100 % water saturation)	26.6
Leachate	0.1
Total	**105.9**
Deficit	15.2 L (12.6 %)

that should be subtracted from the inlet part of the balance). This value was estimated with the mass of methane that was assimilated (6.6 mol of methane removed but not converted to CO_2, based on carbon balance) producing biomass without water formation (net growth of 61.6 $g_{biomass}$, based on a growth yield value of 0.585 $g_{biomass}$ gCH_4^{-1}, according to AlSayed et al., 2018). Additional studies are needed to understand the role of moisture content in the methane biofiltration process.

3.2.5. *Practical implications for improving methane compost biofilters*

Although out of the scope of this work, it is worth mentioning the engineering solutions that have been proposed to reduce the negative effects associated with high temperatures, as discussed above. Several arrangements and devices have been developed aiming to recover heat from compost production (Smith et al., 2017; Fan et al., 2021; Malesani et al., 2021), some of them commercially available. Those include water-jacket tanks, coil tube heat exchangers in the compost bed or at the headspace of the composting unit, percolation water or low temperature technologies using low boiling-point fluids. However, there is scarce information on the application of temperature control devices for biofilters treating gaseous emissions, an issue that deserves further research efforts, especially in the case of compost biofiltration of methane. Possible improvements to enhance methane EC in biofilters may be an in-series vertical arrangement of compost trays of around 30 cm depth, separated by headspaces with coil exchangers and water spraying means; or metallic tubes placed inside the compost bed in a vertical

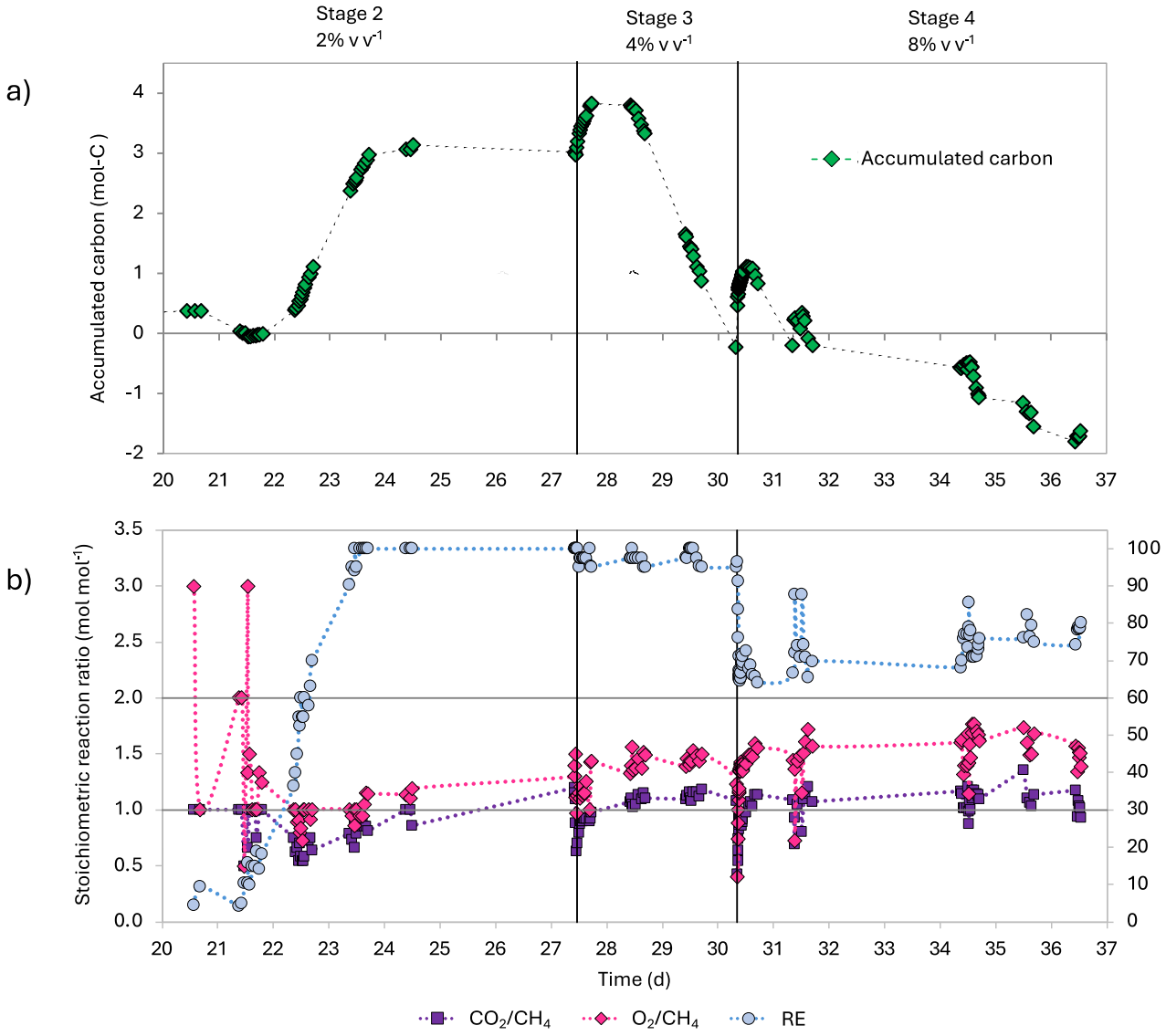

Fig. 7. Evolution of (a) accumulated carbon (resulting from the carbon mass balance at a given time) and (b) stoichiometric reaction ratios and removal efficiency (RE) measured in the compost biofilter during stages 2 to 4.

position acting as heath dissipators or chimney drafts. In this context, effective process control may be achieved through temperature monitoring, acting on the heat exchange rate and moisture addition.

3.3. Carbon fate

A carbon mass balance was used to estimate the fate of carbon in the biofilter, during the experimental period. Methane was utilized for cellular synthesis, resulting in biomass accumulation within the biofilter, and/or oxidized to CO_2. This gas exited the system together with the CO_2 produced by the degradation of additional internal carbon sources, such as cellular reserves (endogenous respiration). Thus, the trend of the accumulated carbon (positive or negative) provides insight into whether the system is primarily incorporating or losing carbon at any given stage. For that purpose and based on the corresponding chemical reaction (Eq. 1), two molar stoichiometric ratios (CO_2/CH_4 and O_2/CH_4) were calculated based on the monitoring results of the outlet gas composition.

Fig. 7a presents the carbon accumulation within the compost biofilter, whereas Fig. 7b shows the evolution of the CO_2/CH_4 and O_2/CH_4 ratios during stages 2 to 4 and the corresponding methane removal efficiency. An interpretation of the combinations of these two representative ratios with the associated possible causes is presented in the supplementary material (Table S2).

As previously mentioned, an acclimation phase of six days was observed for the methanotrophic community, commencing on day 15. But from day 21, the system started to actively remove methane, resulting in the growth of methanotrophic biomass (carbon accumulation) and an increase in CO_2 production and O_2 consumption, with a CO_2/CH_4 ratio starting at 0.5, reaching the stoichiometric value of 1 on day 24. At the same time, the O_2/CH_4 ratio remained between 0.7 and 1.2, below the stoichiometric value of 2. These molar ratios correspond to an intensive cell growth phase, where carbon is being accumulated in the biofilter as new biomass (see Fig. 7a); however, at the end of stage 2, the CO_2/CH_4 ratio was higher than 1, indicating the shift from anabolic to catabolic reactions, while the O_2/CH_4 ratio reached 1.5, still below the stochiometric value of 2. When the methane concentration increased to 4 % (stage 3), the CO_2/CH_4 ratio briefly dropped below 1 before increasing and stabilizing at 1.2 until the end of that stage, as shown in Fig. 7b, indicating that cell growth was favored for a short period (less than 6 h, Fig. 7a) due to more available substrate reaching previously unfed compost (upper) zones. This assumption is supported by the shift in the trend of carbon accumulation (day 28), which finally led to a net carbon release period, from day 31 until the end of the experiment. This behavior may be linked to a microbial community shift from anabolism to catabolism due to temperature increase in this stage (Fig. 5). Under optimal conditions and substrate availability, bacteria tend towards anabolism for growth and replication (stage 2). In contrast, unfavorable conditions, such as extreme temperatures, may prompt a prioritization of catabolic processes to sustain themselves and ensure survival until conditions improve (Dai et al., 2020). Then, it is likely that the synthesized methanotrophic biomass, accumulated during stage 2, once exposed to adverse temperature conditions (around 60 °C in stage 3), switched its metabolism to become mainly catabolic (CO_2 production), making use of their endogenous reserves accompanied by carbon release, explaining the high CO_2/CH_4 ratio (1.2 average value). A similar behavior was registered when methane concentration in the inlet increased to 8 %, represented by a sharp drop in the CO_2/CH_4 ratio, accompanied by a peak of accumulated carbon and temperatures up to 62 °C. However, after this short biomass growth-related behavior, the trend of carbon release persisted, supporting the assumption of metabolic stress due to factors such as the prevailing high temperatures, the reduced gas solubility and the increased drying of the biofilter bed. It is worth mentioning that in stage 4, the average methane removal efficiency was 75 %, indicating that substrate was available in all the compost media, but no additional biomass growth was evidenced due to the referred unfavorable conditions.

3.4. Microbial community analysis

After quality filters, five 16S rRNA gene libraries of 108 to 596 sequences were obtained (see supplementary material, Table S3). The most abundant bacterial groups in the microbial community of the initial compost (IC) and at four different biofilter levels at the end of the experiment are presented in the taxonomic categories of Phylum, Order and Genus (see supplementary material, Fig. S3). During the operation of the biofilter, the initial bacterial community changed at the different levels (L1 to L4). The dendrogram based on the relative abundance of sequences (RAS) at the Phylum taxonomic category shows a change in the structure of the bacterial communities, IC being segregated from the samples taken at the end of the experiment at levels L1, L2, L3 and L4 (see supplementary material, Fig. S3). In the taxonomic category of Genus, there was a clear increase in the RAS of *Methylocaldum* at all levels, unclassified Anaerolineaceae (except L1), S0134_terrestrial_group, and *Steroidobacter* (except L1), while *Sulfurifustis* was identified only at the middle levels of the biofilter (L2 and L3). Genus *Steroidobacter*, AKYG587 and unclassified Gammaproteobacteria and Sutterellaceae were identified only at the end of the experiment, particularly at L4. This was accompanied by a drastic decrease in the relative abundances of bacterial genera such as *Saccharimonadales* and *Cellvibrio*, while *Methylomicrobium* and *Ohtaekwangia* increase their RAS only in L1. Other studies (Milkereit et al., 2021; Wang et al., 2022; Zhang et al., 2020) have reported these bacteria, except Methylomicrobium, in compost and soil (rhizosphere). It is also worth mentioning that the compost-associated genus *Chryseolinea* (Loakasikarn et al., 2021) was among the most abundant in the IC and the biofilter final samples at the four levels.

Their contribution to methane oxidation was assessed based on a bibliographic review of the reported metabolic abilities of the different bacterial genera identified (see supplementary material, Fig. S3; Table 3). In general, it was observed that the most abundant bacteria groups detected in the biofilter can contribute to both assimilative and dissimilative oxidation of intermediates from methane oxidation (formaldehyde and formate). *Chryseolinea* is a genus member of the family Microscillaceae, which, together with the family Anaerolineaceae, have been found in abundance in biofilter samples, comprising chemoheterotrophic bacteria known for degrading complex carbon compounds (Lee et al., 2019; Loakasikarn et al., 2021; Milkereit et al., 2021). The main methanotrophic bacteria in the biofilter were *Methylocaldum* and *Methylomicrobium* (see supplementary material, Fig. S3; Table 3). These bacteria can oxidize methane using the enzymes methane monooxygenase (MMO), methanol dehydrogenase (MDH), and the enzymes of the ribulose monophosphate (RuMP) cycle and serine cycle. In the biofilter, it was observed that *Methylomicrobium* was present only at L1 (temperatures around 45 °C), with a similar abundance than *Methylocaldum* at that level which, however, increased its presence to become the more abundant genus at higher levels (L2 to L4), where temperatures exceeded 50 °C and even 60 °C in level 3 during stages 3 and 4. This predominancy could be due to the thermotolerant capacity of *Methylocaldum* (Smith and Murrell, 2009; Takeuchi et al., 2014) compared to *Methylomicrobium,* which grows mainly under mesophilic conditions (Tikhonova and Kravchenko, 2019). Moreover, assuming that the initial compost contained nitrates (Hoang et al., 2022), *Methylocaldum* and *Sulfurifustis* could contribute to autotrophic denitrification coupled with the oxidation of methane and sulphur, respectively (Qian et al., 2023). Further studies focused on the analysis of genes and metabolites of these bacteria may provide valuable information on the metabolic pathways and adaptive capabilities to thermophilic temperatures and reduced moisture conditions in compost biofilters.

Table 3
Metabolic capabilities of the most abundant bacterial groups in samples of the initial compost (IC) and four levels (L1-L4) of the compost media at the end of the experiment.

Taxonomic assignment at the genus level	Relative abundance of sequences (%)					Metabolic capabilities based on bibliography					References
	IC	L1	L2	L3	L4	MMO and MDH	RuMP	Serine Cycle	DI	Other	
Methylocaldum	2.0	12.2	43.4	25.6	34.3	X	X	X	X	Denitrification	(Cheng et al., 2022; Smith and Murrell, 2009; Takeuchi et al., 2014)
Chryseolinea	7.1	17.1	5.6	8.8	22.2				X	chemoheterotrophic	(Loakasikarn et al., 2021b;
Unclassified Microscillaceae	8.6	18.9	0.0	1.7	0.0				X	chemoheterotrophic	Milkereit et al., 2021)
Unclassified Anaerolineaceae	0.7	0.0	9.9	10.9	3.7				X	chemoheterotrophic	(Loakasikarn et al., 2021b)
Unclassified Actinomarinales	2.5	3.7	7.3	3.4	0.0					*	
Methylomicrobium	0.5	10.4	0.0	0.0	0.0	X	X	Partial	X		(Fu et al., 2017; Yu et al., 2021)
Steroidobacter	0.3	0.0	0.7	4.2	5.6					chemoheterotrophic	(Montecillo, 2023)
Sulfurifustis	0.0	0.0	3.6	5.5	0.0					denitrification and S oxidation	(Qian et al., 2023)
Unclassified Gammaproteobacteria	0.3	0.0	0.0	0.8	6.5					*	
Saccharimonadales	7.4	0.0	0.0	0.0	0.0					chemoheterotrophic	(Wang et al., 2022)
Cellvibrio	6.4	0.0	0.0	0.0	0.0					Chemoheterotrophic Assimilatory sulfate reduction	(Zhang et al., 2020)

Methane oxidation to methanol by methane monooxygenase (**MMO**), methanol oxidation to formaldehyde by methanol dehydrogenase (**MDH**), ribulose monophosphate (**RuMP**) cycle, dissimilation of intermediates (**DI**) (formaldehyde and formate oxidations to CO_2). * The order Actinomarinales and the class Gammaproteobacteria comprise very diverse groups of microorganisms and therefore their possible metabolic roles are also very diverse.

4. Conclusions

The influence of temperature in a pilot-scale compost biofilter under different methane loadings was assessed, achieving over 75 % removal efficiency in thermophilic conditions (>50 °C), attributed to thermotolerant methanotrophs such as *Methylocaldum*. The carbon balance indicated a transition from anabolic biomass growth to catabolism and endogenous respiration, due to the metabolic stress caused by sustained high temperatures (50 to 60 °C). Elevated temperatures adversely affected moisture content within the compost, particularly at the center, creating unfavorable dry conditions for methanotrophic communities. Thus, monitoring and regulation of moisture content are imperative for the stable long-term operation of the system under thermophilic conditions.

CRediT authorship contribution statement

Tania L. Gómez-Borraz: Writing – original draft, Data curation. **Yuly Vanessa Torres-Arévalo:** Writing – original draft, Investigation, Formal analysis. **Yovany Cuetero-Martínez:** Writing – review & editing, Investigation, Formal analysis. **Armando González-Sánchez:** Writing – review & editing, Formal analysis. **Adalberto Noyola:** Writing – review & editing, Supervision, Project administration, Funding acquisition, Formal analysis, Conceptualization.

Declaration of competing interest

The authors declare that they have no known competing financial interests or personal relationships that could have appeared to influence the work reported in this paper.

Acknowledgements

All the experimental work was carried out at the Instituto de Ingeniería of the Universidad Nacional Autónoma de México (UNAM). YTA had financial support from a scholarship provided by CONAHCYT Mexico. The authors thank Margarita E. Cisneros Ortiz and Raúl Robles Cedillo for their technical support. This research did not receive any specific grant from funding agencies in the public, commercial, or not-for-profit sectors.

Appendix A. Supplementary material

Supplementary data to this article can be found online at https://doi.org/10.1016/j.biortech.2025.132097.

Data availability

Data will be made available on request.

References

Agnew, J.M., Leonard, J.J., 2003. The physical properties of compost. Compost Sci Util 11, 238–264. https://doi.org/10.1080/1065657X.2003.10702132.

AlSayed, A., Fergala, A., Khattab, S., Eldyasti, A., 2018. Kinetics of type I methanotrophs mixed culture enriched from waste activated sludge. Biochem Eng J 132, 60–67. https://doi.org/10.1016/j.bej.2018.01.003.

Bian, R., Chen, J., Li, W., Sun, Y., Chai, X., Wang, H., Wang, Y., Zhao, J., 2021. Numerical modeling of methane oxidation and emission from landfill cover soil coupling water-heat-gas transfer: Effects of meteorological factors. Process Safety and Environmental Protection 146, 647–655. https://doi.org/10.1016/j.psep.2020.11.052.

Blakemore, L.C., Searle, P.L., Daly, B.K., 1987. Method for chemical analysis of soils, New Zealand Soil Bureau Scientific. Report.

Bolyen, E., Rideout, J.R., Dillon, M.R., Bokulich, N.A., Abnet, C.C., Al-Ghalith, G.A., Alexander, H., Alm, E.J., Arumugam, M., Asnicar, F., Bai, Y., Bisanz, J.E., Bittinger, K., Brejnrod, A., Brislawn, C.J., Brown, C.T., Callahan, B.J., Caraballo-Rodríguez, A. M., Chase, J., Cope, E.K., Da Silva, R., Diener, C., Dorrestein, P.C., Douglas, G.M., Durall, D.M., Duvallet, C., Edwardson, C.F., Ernst, M., Estaki, M., Fouquier, J., Gauglitz, J.M., Gibbons, S.M., Gibson, D.L., Gonzalez, A., Gorlick, K., Guo, J., Hillmann, B., Holmes, S., Holste, H., Huttenhower, C., Huttley, G.A., Janssen, S., Jarmusch, A.K., Jiang, L., Kaehler, B.D., Kang, K. Bin, Keefe, C.R., Keim, P., Kelley, S. T., Knights, D., Koester, I., Kosciolek, T., Kreps, J., Langille, M.G.I., Lee, J., Ley, R., Liu, Y.X., Loftfield, E., Lozupone, C., Maher, M., Marotz, C., Martin, B.D., McDonald, D., McIver, L.J., Melnik, A. V., Metcalf, J.L., Morgan, S.C., Morton, J.T., Naimey, A. T., Navas-Molina, J.A., Nothias, L.F., Orchanian, S.B., Pearson, T., Peoples, S.L., Petras, D., Preuss, M.L., Pruesse, E., Rasmussen, L.B., Rivers, A., Robeson, M.S., Rosenthal, P., Segata, N., Shaffer, M., Shiffer, A., Sinha, R., Song, S.J., Spear, J.R., Swafford, A.D., Thompson, L.R., Torres, P.J., Trinh, P., Tripathi, A., Turnbaugh, P.J., Ul-Hasan, S., van der Hooft, J.J.J., Vargas, F., Vázquez-Baeza, Y., Vogtmann, E., von Hippel, M., Walters, W., Wan, Y., Wang, M., Warren, J., Weber, K.C., Williamson, C. H.D., Willis, A.D., Xu, Z.Z., Zaneveld, J.R., Zhang, Y., Zhu, Q., Knight, R., Caporaso, J.G., 2019. Reproducible, interactive, scalable and extensible microbiome data

science using QIIME 2. Nature Biotechnology 2019 37:8 37, 852–857. doi: 10.1038/S41587-019-0209-9.
Bonilla-Blancas, W., Garduño-Montero, A., Salazar-Pereyra, M., Gonzalez-Sanchez, A., 2024. Automatic control of water content in a polyurethane foam packed bed used in biotrickling filters for polluted air treatment. J Environ Manage 349. https://doi.org/10.1016/j.jenvman.2023.119554.
Cheng, C., He, Q., Zhang, J., Chen, B., Pavlostathis, S.G., 2022. Is the role of aerobic methanotrophs underestimated in methane oxidation under hypoxic conditions? Science of the Total Environment 833, 155244. https://doi.org/10.1016/j.scitotenv.2022.155244.
Comeau, A.M., Douglas, G.M., Langille, M.G.I., 2017. Microbiome Helper: a Custom and Streamlined Workflow for Microbiome Research. mSystems 2. doi: 10.1128/MSYSTEMS.00127-16/ASSET/38C6CF12-8D9A-4C92-A8F5-F0B92BC4EE7B/ASSETS/GRAPHIC/SYS0011720760005.JPEG.
Dai, Z., Yu, M., Chen, H., Zhao, H., Huang, Y., Su, W., Xia, F., Chang, S.X., Brookes, P.C., Dahlgren, R.A., Xu, J., 2020. Elevated temperature shifts soil N cycling from microbial immobilization to enhanced mineralization, nitrification and denitrification across global terrestrial ecosystems. Glob Chang Biol 26, 5267–5276. https://doi.org/10.1111/gcb.15211.
Fan, S., Li, A., ter Heijne, A., Buisman, C.J.N., Chen, W.S., 2021. Heat potential, generation, recovery and utilization from composting: A review. Resources, Conservation and Recycling 175, 105850. https://doi.org/10.1016/j.resconrec.2021.105850.
Fjelsted, L., Scheutz, C., Christensen, A.G., Larsen, J.E., Kjeldsen, P., 2020. Biofiltration of diluted landfill gas in an active loaded open-bed compost filter. Waste Management 103, 1–11. https://doi.org/10.1016/j.wasman.2019.12.005.
Fu, Y., Li, Y., Lidstrom, M., 2017. The oxidative TCA cycle operates during methanotrophic growth of the Type I methanotroph Methylomicrobium buryatense 5GB1. Metab Eng 42, 43–51. https://doi.org/10.1016/j.ymben.2017.05.003.
Gómez-Borraz, T.L., González-Sánchez, A., Bonilla-Blancas, W., Revah, S., Noyola, A., 2017. Characterization of the biofiltration of methane emissions from municipal anaerobic effluents. Process Biochemistry 63, 204–213. https://doi.org/10.1016/j.procbio.2017.08.011.
Gómez-Borraz, T.L., González-Sánchez, A., Cabello, J., Noyola, A., 2022. Model assessment on the non-isothermal methane biofiltration at ambient conditions. Process Safety and Environmental Protection 163, 283–297. https://doi.org/10.1016/j.psep.2022.05.042.
Gomez-Cuervo, S., Hernandez, J., Omil, F., 2016. Identifying the limitations of conventional biofiltration of diffuse methane emissions at long-term operation. Environ Technol 37, 1947–1958. https://doi.org/10.1080/09593330.2015.1135996.
Hettiarachchi, V.C., Hettiaratchi, P.J., Mehrotra, A.K., Kumar, S., 2011. Field-scale operation of methane biofiltration systems to mitigate point source methane emissions. Environmental Pollution 159, 1715–1720. https://doi.org/10.1016/j.envpol.2011.02.029.
Hoang, H.G., Thuy, B.T.P., Lin, C., Vo, D.V.N., Tran, H.T., Bahari, M.B., Le, V.G., Vu, C.T., 2022. The nitrogen cycle and mitigation strategies for nitrogen loss during organic waste composting: A review. Chemosphere 300, 134514. https://doi.org/10.1016/j.chemosphere.2022.134514.
Huber-Humer, M., Röder, S., Lechner, P., 2009. Approaches to assess biocover performance on landfills. Waste Management 29, 2092–2104. https://doi.org/10.1016/j.wasman.2009.02.001.
Huete, A., de los Cobos-Vasconcelos, D., Gómez-Borraz, T., Morgan-Sagastume, J.M., Noyola, A., 2018. Control of dissolved CH4 in a municipal UASB reactor effluent by means of a desorption – Biofiltration arrangement. J Environ Manage 216, 383–391. doi: 10.1016/j.jenvman.2017.06.061.
Ipcc, 2021. Climate Change 2021 – The Physical Science Basis, Climate Change 2021 – The Physical Science Basis. Cambridge University Press, Cambridge, United Kingdom and New York, NY, USA. https://doi.org/10.1017/9781009157896.
Lee, S.A., Kim, Y., Sang, M.K., Song, J., Kwon, S.W., Weon, H.Y., 2019. Chryseolinea soli sp. nov., isolated from soil. Journal of Microbiology 57, 122–126. https://doi.org/10.1007/s12275-019-8562-4.
Loakasikarn, T., Kubota, Y., Koyama, M., Nakasaki, K., 2021. Effect of seeding materials on organic matter degradation and microbial community succession during model organic waste composting. Biocatal Agric Biotechnol 37, 102182. https://doi.org/10.1016/j.bcab.2021.102182.
Malesani, R., Pivato, A., Bocchi, S., Lavagnolo, M.C., Murano, S., Schievano, A., 2021. Compost heat recovery systems: An alternative to produce renewable heat and promoting ecosystem services. Environmental Challenges 4, 100131. https://doi.org/10.1016/j.envc.2021.100131.
Milkereit, J., Geisseler, D., Lazicki, P., Settles, M.L., Durbin-Johnson, B.P., Hodson, A., 2021. Interactions between nitrogen availability, bacterial communities, and nematode indicators of soil food web function in response to organic amendments. Applied Soil Ecology 157, 103767. https://doi.org/10.1016/j.apsoil.2020.103767.
Montecillo, J.A.V., 2023. Phylogenomics and molecular marker-based analyses of the order Nevskiales: proposal for the creation of Steroidobacterales ord. nov. and Peristeroidobacter gen. nov. Res Microbiol 174, 104057. https://doi.org/10.1016/J.RESMIC.2023.104057.
Morales, M., Hernandez, S., Cornabe, T., Revah, S., Auria, R., Hernández, S., Cornabé, T., 2003. Effect of drying on biofilter performance: Modeling and experimental approach. Environ Sci Technol 37, 985–992. https://doi.org/10.1021/es025970w [doi].
Morgan-Sagastume, J.M., Noyola, A., Revah, S., Ergas, S.J., 2003. Changes in physical properties of a compost biofilter treating hydrogen sulfide. J Air Waste Manag Assoc 53, 1011–1021. https://doi.org/10.1080/10473289.2003.10466249.
Nikiema, J., Bibeau, L., Lavoie, J., Brzezinski, R., Vigneux, J., Heitz, M., 2005. Biofiltration of methane: An experimental study. Chemical Engineering Journal 113, 111–117. https://doi.org/10.1016/j.cej.2005.04.005.
Pearce, D., 2023. Ecology of methanotrophs in a landfill methane biofilter.
Qian, L., Yu, X., Gu, H., Liu, F., Fan, Y., Wang, C., He, Q., Tian, Y., Peng, Y., Shu, L., Wang, S., Huang, Z., Yan, Q., He, J., Liu, G., Tu, Q., He, Z., 2023. Vertically stratified methane, nitrogen and sulphur cycling and coupling mechanisms in mangrove sediment microbiomes. Microbiome 2023 11:1 11, 1–19. doi: 10.1186/S40168-023-01501-5.
Quast, C., Pruesse, E., Yilmaz, P., Gerken, J., Schweer, T., Peplies, J., Yarza, P., Glöckner, F.O., 2013. The SILVA ribosomal RNA gene database project : improved data processing and web-based tools. Nucleic Acids Res 41, 590–596. https://doi.org/10.1093/nar/gks1219.
Salahudeen, N., Rasheed, A.A., Babalola, A., Moses, A.U., 2022. Review on technologies for conversion of natural gas to methanol. J Nat Gas Sci Eng 108, 104845. https://doi.org/10.1016/j.jngse.2022.104845.
Saunois, M., Stavert, A., Poulter, B., Bousquet, P., Canadell, J.G., Jackson, R.B., Raymond, P.A., Dlugokencky, E.J., Houweling, S., Patra, P.K., Ciais, P., Arora, V.K., Bastviken, D., Bergamaschi, P., Blake, D.R., Brailsford, G., Bruhwiler, L., Carlson, K.M., Carrol, M., Castaldi, S., Chandra, N., Crevoisier, C., Crill, P.M., Covey, K., 2020. The global methane budget. Earth Syst Sci Data 12, 1561–1623.
Scheutz, C., Cassini, F., De Schoenmaeker, J., Kjeldsen, P., 2017. Mitigation of methane emissions in a pilot-scale biocover system at the AV Miljø Landfill, Denmark: 2. Methane Oxidation. Waste Management 63, 203–212. https://doi.org/10.1016/j.wasman.2017.01.012.
Smith, M.M., Aber, J.D., Rynk, R., 2017. Heat recovery from composting: A comprehensive review of system design, recovery rate, and utilization. Compost Science & Utilization 51, 511–522. https://doi.org/10.1080/1065657X.2016.1233082.
Smith, T.J., Murrell, J.C., 2009. Methanotrophy/methane oxidation Defining Statement Introduction Ecology and Taxonomy of Methanotrophs Physiology and Biochemistry of Methanotrophs Methanotrophs in Biotechnology Postgenomics of Methanotrophs Further Reading. Environmental Microbiology and Ecology 293–298.
Stein, V.B., Hettiaratchi, J.P., 2001. Methane oxidation in three Alberta soils: influence of soil parameters and methane flux rates. Environ Technol 22, 101–111. https://doi.org/10.1080/09593332208618315.
Streese, J., Stegman, R., 2003. Microbial oxidation of methane from old landfills in biofilters. Waste Manag. 23, 573–580. https://doi.org/10.1016/S0956-053X(03)00097-7.
Takeuchi, M., Kamagata, Y., Oshima, K., Hanada, S., Tamaki, H., Marumo, K., Maeda, H., Nedachi, M., Hattori, M., Iwasaki, W., Sakata, S., 2014. Methylocaldum marinum sp. nov., A thermotolerant, Methane-oxidizing bacterium isolated from marine sediments, And emended description of the genus methylocaldum. Int J Syst Evol Microbiol 64, 3240–3246. https://doi.org/10.1099/ijs.0.063503-0.
Tikhonova, E.N., Kravchenko, I.K., 2019. Activity and diversity of aerobic methanotrophs in thermal springs of the russian far east, New and Future Developments in Microbial Biotechnology and Bioengineering: Microbial Biotechnology in Agro-environmental Sustainability. Elsevier B.V. doi: 10.1016/B978-0-444-64191-5.00001-8.
Turgeon, N., le Bihan, Y., Buelna, G., Bourgault, C., Verreault, S., Lessard, P., Nikiema, J., Heitz, M., 2011. Application of methanotrophic biofilters to reduce GHG generated by landfill in Quebec City (Canada). WIT Transactions on Ecology and the Environment 147, 387–397. https://doi.org/10.2495/AIR110361.
van Lith, C., Leson, G., Michelsen, R.F., 1997. Evaluating design options for biofilters. J Air Waste Manage Assoc 47, 37–48. https://doi.org/10.1080/10473289.1997.10464410.
Wang, G., Jin, Z., Wang, X., George, T.S., Feng, G., Zhang, L., 2022. Simulated root exudates stimulate the abundance of Saccharimonadales to improve the alkaline phosphatase activity in maize rhizosphere. Applied Soil Ecology 170, 104274. https://doi.org/10.1016/j.apsoil.2021.104274.
Yu, G., Wang, M., Zhang, C., Ma, Z., Zhang, H., Mo, X., Sun, Y., Xing, X., Yang, S., 2021. Production of high value-added chemicals by engineering methylotrophic cell factories. Microbial Cell Factories Engineering for Production of Biomolecules 265–276. https://doi.org/10.1016/B978-0-12-821477-0.00016-7.
Zhang, Y., Xu, J., Wang, E., Wang, N., 2020. Mechanisms Underlying the Rhizosphere-To-Rhizoplane Enrichment of Cellvibrio Unveiled by Genome-Centric Metagenomics and Metatranscriptomics. Microorganisms 2020, Vol. 8, Page 583 8, 583. doi: 10.3390/MICROORGANISMS8040583.